Journal of Materials Chemistry B

ROYAL SOCIETY OF CHEMISTRY

PAPER

View Article Online
View Journal

Cite this: DOI: 10.1039/d1tb01164b

Synthesis, characterization and use of enzyme cashew gum nanoparticles for biosensing applications†

Adriany das Graças Nascimento Amorim, ‡[a] Marta Sánchez-Paniagua,‡[b] Taiane Maria de Oliveira,[a] Ana Carolina Mafud,[c] Durcilene Alves da Silva,[a] José Roberto de Souza de Almeida Leite[d] and Beatriz López-Ruiz *[b]

Received 24th May 2021,
Accepted 2nd August 2021

DOI: 10.1039/d1tb01164b

rsc.li/materials-b

This research reports, for the first time, the immobilization of an enzyme - *Rhus vernificera* laccase - on cashew gum (CG) nanoparticles (NPs) and its application as a biological layer in the design and development of an electrochemical biosensor. Laccase-CG nanoparticles (LacCG-NPs) were prepared by the nanoprecipitation method and characterized by UV-Vis spectrophotometry, atomic force microscopy, scanning electron microscopy, attenuated total reflectance-Fourier-transform infrared spectroscopy, circular dichroism, cyclic voltammetry, and electrochemical impedance spectroscopy. The average size and stability of the NPs were predicted by DLS and zeta potential. The ATR-FTIR results clearly demonstrated an interaction between –NH and –OH groups to form LacCG-NPs. The average size found for LacCG-NPs was 280 ± 53 nm and a polydispersity index of 0.309 ± 0.08 indicated a good particle size distribution. The zeta potential shows a good colloidal stability. The use of a natural product to prepare the enzymatic nanoparticles, its easy synthesis and the immobilization efficiency should be highlighted. LacCG-NPs were successfully applied as a biolayer in the development of an amperometric biosensor for catechol detection. The resulting device showed a low response time (6 s), good sensitivity (7.86 μA μM^{-1} cm^{-2}), wide linear range of 2.5×10^{-7}–2.0×10^{-4} M, and low detection limit (50 nM).

1. Introduction

Laccases (benzenediol: oxygen oxidoreductases) are copper-containing enzymes, produced by several species of bacteria, fungi, plants, and some insects, being particularly abundant in white-rot basidiomycetes.[1–4] These enzymes can be used to catalyze the oxidation of *ortho* and *para*-diphenols, such as catechol[2,5] and many polyphenol compounds, to the corresponding quinone, as well as aromatic amines with the simultaneous reduction of molecular oxygen to water, which is the final electron acceptor of such reactions.[2,3]

However, the relatively low stability of free-laccase[5–7] hinders its large-scale application and, therefore, studies have been performed to immobilize laccase in nanosystems.[8,9] These nanosystems comprise different types of nanoparticles, such as polymer nanoparticles[10,11] which have several applications and can improve the stability of this protein.

Immobilized enzymes have been widely used in the pharmaceutical, chemical, textile, and food industry, as well as in the environmental and biomedical areas, with multiple applications, such as biosensors, biofuel cells, biocatalysis, and bioremediation processes to green synthesis.[6–8] Similarly, methods of enzyme immobilization based on nanoparticles have shown substantial advantages,[9] such as high density of enzymatic charge, better stability, and easy separation of the reaction products, as well as the possibility to synthesize nanoparticles without the use of surfactants or toxic reagents. Also, well-defined and homogeneous nanoparticles can be obtained once the size of the nanoparticles can be conveniently adapted to practical needs.[7,8,12]

The characteristic large surface area of nanomaterials provides a homogeneous structure that allows easy access to the active groups of the enzyme.[9] These nanoparticles, with sizes between 10–1000 nm, can be synthesized from both

[a] *Biodiversity and Biotechnology Research Center, Federal University of Piaui, 64202-020, Parnaiba-PI, Brazil*
[b] *Chemistry in Pharmaceuticals Sciences Department, Faculty of Pharmacy, Complutense University of Madrid, Ciudad Universitaria, 28240, Madrid, Spain. E-mail: bealopru@ucm.es*
[c] *São Carlos Institute of Physics, University of São Paulo, USP, São Carlos, 13565-905, São Paulo, Brazil*
[d] *Morphology Area, Faculty of Medicine, University of Brasília (UnB), Campus Darcy Ribeiro, Asa Norte, Brasília-DF, 70910-900, Brazil*

† Electronic supplementary information (ESI) available. See DOI: 10.1039/d1tb01164b

‡ These authors have contributed equally to this work.

synthetic and natural polymers, such as lipids, proteins, and carbohydrates.[10,13,14] The enzyme covalent immobilization, in both organic and inorganic polymers, results in the irreversible binding of the enzyme to the support matrix.[7,12,13]

Cashew gum (CG) is a natural hydrophilic biopolymer with multiple advantages, such as low cost, biocompatibility, and self-assembly in water, forming nanoparticles or nanogels through nanoprecipitation or other methods.[10,11,14,15] For this reason, it is useful for applications in different fields of the pharmaceutical and biotechnology industries as thickeners, emulsifiers, viscosifiers, sweeteners, and, more recently, in nanotechnologies and controlled drug release.[10,16]

Literature has already reported the use of CG polymer in the immobilization process of peroxidase.[17] Besides, polymeric nanoparticle systems have been explored either for electron transfer with enzymes or bioelectrocatalysis.[18] The immobilization of laccase on different types of nanoparticles, such as chitosan nanoparticles, nanotubes, and magnetics nanoparticles, has also been described.[19] However, to our knowledge, the immobilization of enzymes on cashew gum nanoparticles and the use of these nanostructures in biosensors design have not been described yet.

Thus, we performed the present study aiming to use cashew gum nanoparticles as an immobilization enzyme system. The laccase-CG nanoparticles were synthesized by a nanoprecipitation method and characterized by dynamic light scattering (DLS), zeta potential, UV-visible absorption spectroscopy, attenuated total reflectance-Fourier-transform infrared spectroscopy (ATR-FTIR), circular dichroism (CD), atomic force microscopy (AFM), scanning electron microscopy (SEM), and electrochemical methods, such as cyclic voltammetry and electrochemical impedance spectroscopy. The applicability of these nanoparticles as the biological component in the design of an electrochemical biosensor was explored.

2. Materials and methods

2.1 Reagents

Laccase from *Rhus vernificera* (crude acetone powder, ≥50 units per mg – solid) and catechol (95%) were purchased from Sigma-Aldrich. Potassium ferrocyanide trihydrate (98%) was purchase from Fluka. Acetone (99%) and ethanol (96° G.L.) were obtained from Spectrum Medical Industries. The buffer solutions were prepared using disodium monohydrogen phosphate (99%), sodium dihydrogen phosphate (99%) and sodium acetate (99%) (Panreac). All materials were used without further purification. The water used for all the experiments was obtained with a Milli-Q ultrapure system (Millipore).

2.2 Isolation and purification of cashew gum (CG)

Cashew gum was collected from *Anacardium occidentale* L. trees grown at Ilha Grande de Santa Isabel – Piaui/Brazil (Latitude: 2°51′57″S, Longitude: 41°48′42″W), between August and November/2016. The polysaccharide was purified according to the method described by Amorim *et al.*[20] The gum was ground and suspended in ultrapure water (Milli-Q). The material was filtered and precipitated with commercial ethanol (96 °GL) at ethanol : gum 3 : 1 (w/w) ratio. The precipitate was isolated and dried at 60 °C using a hot airflow. After purification, CG samples were solubilized in ultrapure water, under stirring for 2 h, and filtered through a sintered glass, under vacuum. Finally, the gum was crushed in a mill, resulting in a fine white powder. The molar mass of CG was estimated using gel permeation chromatography (GPC).

2.3 Synthesis of Laccase cashew gum nanoparticles (LacCG-NPs)

The synthesis of Laccase-cashew gum nanoparticles was performed using the nanoprecipitation method described by

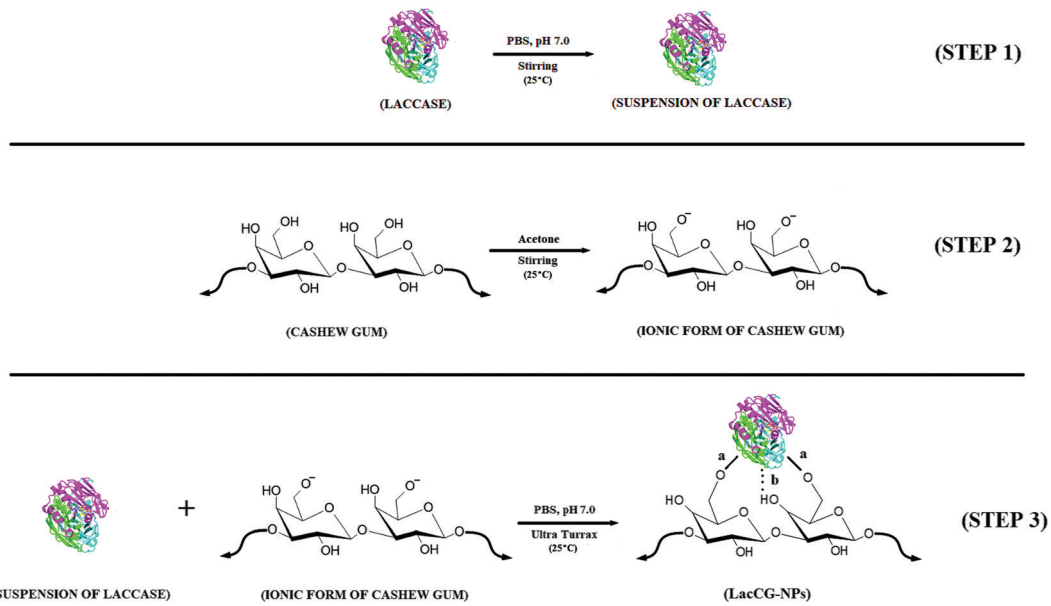

Scheme 1 Schematic illustration of LacCG-NPs synthesis.

Dias *et al.*[11] with minor modifications. LacCG-NPs were prepared by adding laccase to the aqueous phase, using the following protocol. A solution of cashew gum in acetone (0.1% w/v) and a suspension of laccase in phosphate buffered solution (PBS) at pH 7.0 (0.05%, w/v and 0.01%, w/v) were prepared. Subsequently, 10 mL of the laccase suspension was incorporated into 10 mL of the CG solution and homogenized by Ultra Turrax (T25 Basic Heidolpha) at 15 000 rpm for 5 min. The acetone was removed by evaporation in a Heidolph Rzr205 rotary evaporator system at 25 °C for 10 min. LacCG-NPs were synthesized with CG : laccase ratios of 10 : 5 or 10 : 1. LacCG-NPs were stored under refrigeration in a falcon tube for further characterization. Scheme 1 illustrates the synthesis of LacCG-NPs.

2.4 Biosensor preparation

The glassy carbon electrode surface ($\varnothing$ = 3 mm) was polished with alumina slurry paste (0.05 mm and 0.1 mm) and any residual abrasive particle was rinsed with ethanol and water. A volume of the LacCG-NPs suspension was spread on the glassy carbon electrode surface and the coating was dried in air at room temperature for 1 h. Finally, the LacCG-NPs biolayer was hydrated for 20 min in a 0.1 M PBS (pH 7.0).

2.5 Apparatus and measurements

For the molar mass estimation a linear PolySep (300 × 7.8 mm) column for size exclusion separations coupled to a refractive index detector (Waters 2414) was used. An injection volume of 50 μL was loaded, the flow rate was 0.8 mL min^{-1} (30 °C), and 0.1 mol L^{-1} $NaNO_3$ (aq.) was used as the eluent. The calibration curve was elaborated from the logarithm of the molar mass ($\log M_w$) of the Shodex Pullulan standard (M_w = 5000–642 000 Da, NY, USA) for GPC, and their respective elution volumes (Fig. S1, ESI†). Through the resulting equation and the elution volume (V_e) of the GC, its Mw in g mol^{-1} was calculated:

$$\log M_w = 14.40038 - 0.50852 \times V_e,\ R^2 = 0.98926 \quad (1)$$

The UV-Vis absorption spectra of laccase, CG-NPs, and LacCG-NPs were obtained with a Shimadzu Spectrophotometer UV-1800, between 190 nm and 750 nm. All measurements were performed in triplicate at 25 °C. DLS for distribution measurements and zeta potential of the nanoparticles in suspension were performed in a Zetasizer Nano – ZS90 (Malvern Instruments, UK), using laser diffraction with equilibration for 2 minutes at 25 °C before the measurements. Three measurements per sample were performed, and the results were expressed as mean ± SD.

The characterization of LacCG-NPs was investigated using an IRAffinity-1S FTIR Spectrophotometer (Shimadzu) with the attenuated total reflectance (ATR) technique, over the range 4000 to 700 cm^{-1}. The samples were placed on a Zinc selenide ATR crystal, and their spectra were collected. LacCG-NPs spectrum was compared with the spectra of purified CG-NPs and laccase.

The morphological characterization of the nanoparticles was carried out by the AFM technique (Bruker Dimension ICON AFM), in tapping mode, using cantilevers with integral tips at resonant frequency of approximately 300 kHz. Images were analyzed using the Gwyddion software. The morphology of CG-NPs and LacCG-NPs was also analyzed by scanning electron microscopy (SEM) JEOL JSM-IT300, Tokio, Japan. A secondary electron detector with an accelerating voltage of 8 kV was applied. A drop of the nanoparticle solution was deposited onto different glass slides and dried in a desiccator. Then, replicas were produced by shadowing with gold under vacuum. The average particle size was determined using the Fiji software after individual measures of different fields.

The measurement of CD mobility was simulated at t = 30 °C, μ = 10 000 cm^2 V^{-1}, in the range of 180 to 260 nm for 1 h of incubation, in a Jasco-J810 Spectropolarimeter (Jasco, Easton, MD). The analysis was performed for CG-NPs and LacCG-NPs, with a laccase : cashew gum ratio of 10 : 5.

The electrochemical measurements were carried out with a μ-Autolab PGSTAT12 potentiostat, with NOVA 2.1 software (EcoChemia, The Netherlands), connected to a three-electrode cell with a modified glassy-carbon working electrode, a platinum counter electrode, and an Ag/AgCl 3 M reference electrode. All the experimental electrochemical measurements were carried out in a thermostated cell containing 10 mL of phosphate buffer solution. Amperometric measurements were carried out at a constant potential *versus* Ag/AgCl 3 M electrode in a stirred electrolyte solution when the steady state was reached. The linear region of the calibration plots was fixed according to the best correlation coefficient (R^2). The sensitivity was expressed as the slope of these plots. The response time was determined as the time required to reach 95% of the current and the detection limit was obtained following IUPAC recommendation by the analysis of ten blank samples.

Cyclic voltammetry was performed at 100 mV s^{-1}, in a potential range from −0.4 V to 1.0 V, using $K_4[Fe(CN)_6]$ 1 mM as the redox probe. Electrochemical impedance spectroscopy, useful for studying the interface properties of surface-modified electrodes, was performed in a frequency range of 10 kHz to 0.1 Hz, under 5 mV excitation at open-circuit potential.

3. Results and discussion

3.1 UV-Vis characterization

As described in literature, UV-Vis spectroscopy is a primary technique for the characterization of polymeric nanoparticles, as well as for purified laccase.[5,21,22] Therefore, characterization by UV-vis spectroscopy was performed by comparing the absorbance spectra of laccase, CG-NPs, and LacCG-NPs, as shown in Fig. 1. Both CG-NPs and LacCG-NPs showed a peak at 262 nm while laccase shows a shoulder peak around 327 nm, which has been reported as a type III binuclear Cu(II) complex cluster,[3,5,22,23] responsible for electron transference and the reduction of oxygen to produce water molecules.[3,4]

We observed that CG-NPs showed an absorbance close to 0 at 300 nm and above, while LacCG-NPs showed an absorbance around 0.1 which could be attributed to the presence of laccase. Besides, both laccase and LacCG-NPs in suspension presented a yellow color as a result of the spectral characteristics of type

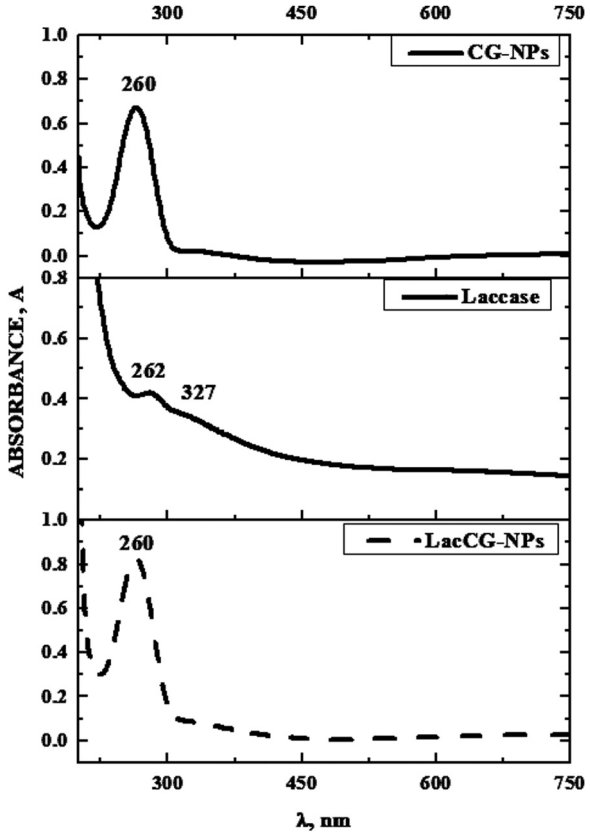

Fig. 1 UV-Vis spectra of Laccase, CG-NPs, and LacCG-NPs (CG : laccase ratio of 10 : 5) in PBS (0.1 M; pH 7.0).

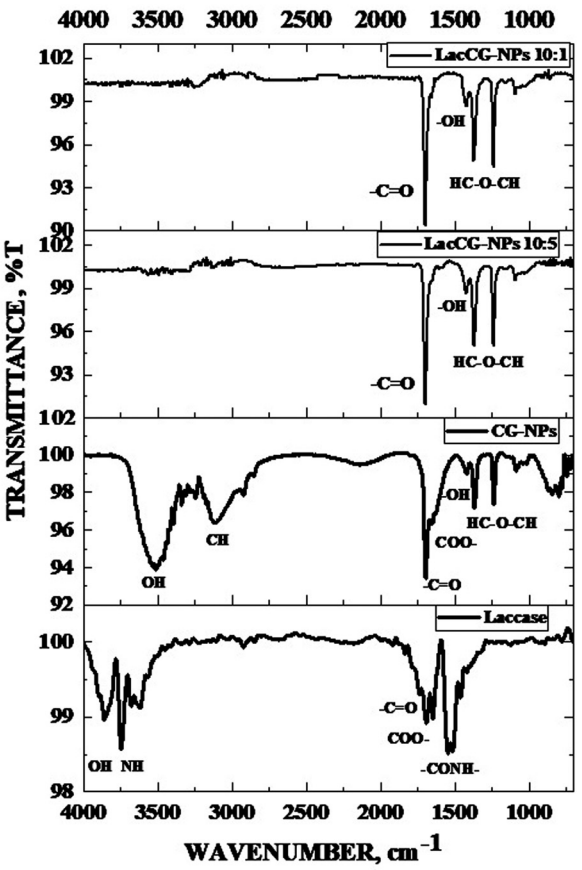

Fig. 2 Attenuated total reflectance Fourier-transform infrared spectroscopy spectra of Laccase, CG-NPs, and LacCG-NPs. CG : laccase ratio of 10 : 5 and 10 : 1, suspended in PBS (0.1 M; pH 7.0).

III binuclear Cu(II) complex,[3,22] which has a total of six histidine ligands.[4]

3.2 ATR-FTIR study

To identify the possible interactions between laccase and cashew gum during the process of nanoparticle formation, we performed an ATR-FTIR characterization, once ATR is often the method of choice for aqueous solutions or viscous liquids analysis. To obtain the spectra, CG-NPs and LacCG-NPs (CG : Laccase ratios of 10 : 5 and 10 : 1) were suspended in PBS (pH 7.0) and analyzed (Fig. 2).

The ATR-FTIR spectrum of laccase showed some peaks at higher wavenumbers, around 4000–3500 cm^{-1}. One of these peaks corresponds to a characteristic stretching of the –OH group and the other to –NH group from secondary amines, present in protein molecules.[6–8,12] Confirming the presence of these functional groups in the structure of laccase suggests that they can be the active sites used for binding to other molecules, such as carbohydrate polymers.[12] Moreover, the band at 1650 cm^{-1}, which corresponds to –CONH– in laccase structure, is also characteristic of proteins.[7,24] It is associated with an amide band derived mainly from the C═O stretching vibration of the peptide linkages in laccase.[1,24] The bands at 1547 cm^{-1} and 1518 cm^{-1} were assigned to –NH bending vibration and –CN stretching vibration of amide in laccase.[1] The peaks at 1694 and 1738 cm^{-1}, in turn, were attributed to C═O and COO^- stretching, respectively, confirming the exposure of carboxyl side groups from the amino acid residues of the α and β fractions of the secondary structure of laccase.[6,8,24] Thus, all the chemical groups that are usually found in the FTIR characterization of protein molecules were also present in the spectrum of laccase, as observed in this study.

On the other hand, the broadband identified between 3370 cm^{-1} and 3660 cm^{-1} in the spectrum of the CG-NPs was attributed to the O–H vibrational state of intermolecular bonded alcohol, typical of the cashew gum structure, and to the scissor stretching of OH from water molecules of PBS.[10,16,20,25–27] Another broadband of asymmetric stretching was observed between 2920 cm^{-1} and 3100 cm^{-1}, and was associated with C–H commonly found in cashew gum when its structure is analyzed by ATR-FTIR.[10,16,20,25–27] Besides, the asymmetric vibration at 1695 cm^{-1} is attributed to the C═O stretching vibration of carboxylic acid groups due to the presence of the glucuronic acid in CG.[17,26] The water bending mode through O–H scissor vibrations[14,15,17,26] corresponds to the signal between 1680–1550 cm^{-1} in an asymmetric stretching and was attributed to the COO^- of carboxylic acid in CG structure.[15,27] The glycosidic –OH stretching vibration was correlated with the peak at 1422 cm^{-1}.[26] The peaks at 1369, 1238, and 1092 cm^{-1}, in turn, were attributed to the –CO

stretching vibrations of the glycosidic linkages HC–O–CH of the polysaccharide[10,16,20,25–27] and to the bending vibrations of –OH from alcohols of the pyranosidic structures of CG.[14–17,20,26]

It is noteworthy that the bands between 3500 and 4000 cm^{-1} in the spectra of LacCG-NPs should have increased absorbance due to the additive effect of the signals derived from the –OH groups of CG with the signals from the –OH and –NH groups of laccase. Nevertheless, we observed that these bands disappeared. These results suggest that the chemical treatment involved in the synthesis of the NPs leads to the formation of covalent bonds and, therefore, to a structural modification (Fig. 2).

The same behaviour was observed for the peaks at higher wavenumbers in the spectrum of laccase. Therefore, the ATR-FTIR spectra confirmed that NH and OH groups are responsible for the main connection between laccase and CG to form LacCG-NPs.[8,12] These data can be attributed to the disruption of the hydrogen bonds of the enzyme and the formation of new hydrogen bonds between laccase and cashew gum[7,28] once NH and OH groups are easily used in bioconjugation and/or immobilization as a positive effect[12] to modify other molecules or to form nanomaterials.[8]

Besides, the band associated with the vibrations of the –CONH– group from laccase was fully covered by the peaks close to 1238, 1369, and 1697 cm^{-1} of CG due to the strong interaction between the amino groups of the enzyme with the polysaccharide.[9] A highly symmetrical peak at 1697 cm^{-1} indicated that –C═O from carboxylic acid groups[15] are more exposed and may contribute to increase the zeta potential of LacCG-NPs, and the non-appearance of new peaks in its IR indicated the laccase was incorporated in the NPs.[7,28]

3.3 Microscopy assays

AFM images show the morphological characterization of CG-NPs and LacCG-NPs (Fig. 3E and F). These nanoparticles appear to be spherical with a homogeneous distribution.[10,29] The results from AFM and DLS do not agree with each other (Table 1). AFM images are obtained with dry nanoparticles, while in DLS, aqueous dispersions of NPs are used. As expected, the radius of the dry particle obtained by AFM was smaller than the hydrodynamic radius obtained by DLS since the ionic layers, the solvation layer, and the dispersion/aggregation of the nanoparticles in the solution are considered in the latter technique.[10,29,30] SEM images of the nanoparticles without and with the enzyme (CG-NPs and LacCG-NPs) are represented in Fig. 3A and B, respectively. These images demonstrate smooth and uniform surfaces for both nanoparticles, which have in general globular shapes and a homogeneous diameter

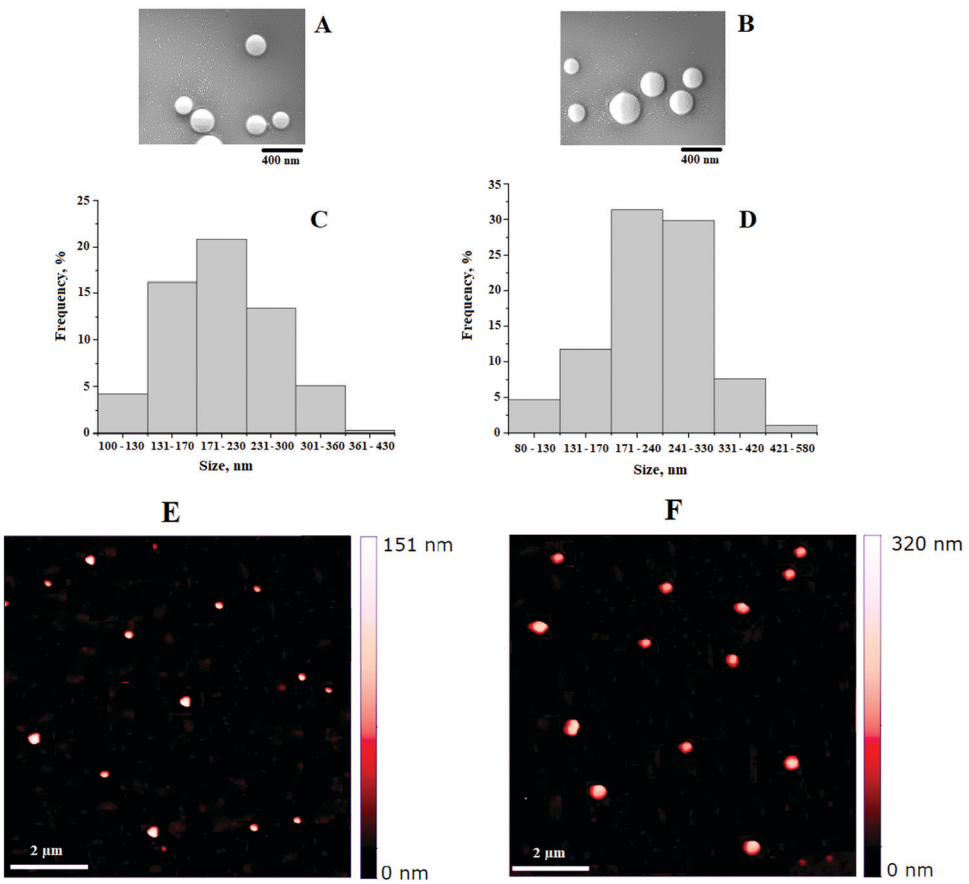

Fig. 3 SEM micrograph of CG-NPs (A) and LacCG-NPs (B). Frequency histogram of CG-NPs (C) and LacCG-NPs (D) diameter distribution. Atomic force microscopy of CG-NPs (E) and LacCG-NPs (F).

Table 1 Characterization of cashew gum nanoparticles produced by nanoprecipitation

	Size (nm)				
Nanoparticle	AFM	SEM	DLS	PDI	ζ (mV)
CG-NPs	116 ± 27	176 ± 18	225 ± 10	0.287 ± 0.05	−3.73 ± 0.29
LacCG-NPs	167 ± 46	215 ± 38	280 ± 53	0.309 ± 0.08	−10.86 ± 0.50

distribution (Fig. 3C and D). Table 1 shows the average particle size obtained by AFM and SEM for both nanoparticles. Based on these data, no drastic changes were observed on the NPs after the incorporation of the enzyme, except for a slight increase in size.[31]

3.4 Dynamic light scattering and zeta potential test

The polymeric nanoparticles with and without laccase were obtained by nanoprecipitation and characterized according to the average hydrodynamic size, polydispersity index (PDI), and zeta potential. DLS provided the size of the CG-NPs and LacCG-NPs. This technique is used for measuring the size of particles typically in the submicron region, such as the nanoparticles produced with polymer molecules in this study. The average hydrodynamic size of the synthesized LacCG-NPs measured by DLS was 280 ± 53 nm and a PDI of 0.309 ± 0.08 (Fig. S2, ESI†), while CG nanoparticles without enzyme presented an average hydrodynamic size of 225 ± 10 nm and a PDI of 0.287 ± 0.05 (Fig. S3, ESI†).

The molar mass of CG was also calculated by GPC The elution volume (V_e) of CG was 19.7 mL. The molar mass (M_w) of CG was calculated from this volume by calibration curve (Fig. S1, ESI†). A molar mass M_w around 2.41×10^4 g mol^{-1} was established. Polydispersity index (PDI) of 2.56 that are in according with those described in the literature.[10,25,26]

The sizes of CG-NPs and LacCG-NPS corroborated the data described in the literature for the sizes observed for cashew gum nanoparticles[14,15,25,27] with or without structural changes and produced by nanoprecipitation.[10]

As shown in Table 1, the PDI observed for cashew gum nanoparticles with and without laccase indicated a good particle size distribution. The lowest PDI found for CG-NPs indicates incorporating laccase in the nanoparticles makes their particle size uniform and more homogeneous.[10,25,27]

The zeta potentials of CG-NPs and LacCG-NPs were determined because this physical property can be used for predicting the stability and the possibility of aggregation for particles in suspension. CG-NPs presented a zeta potential of −3.73 ± 0.29 mV.[25] These values may be associated with the presence of carboxylic acid groups (COO^-) in the cashew gum structure[15] once polysaccharides purified from gum exudates have anionic characteristics.[32] When a complex structure as laccase interacts with CG to form nanoparticles (LacCG-NPs) a slight increase in zeta potential to more negative values is observed[24,25] (Table 1). Zeta potential is a parameter used to characterize nanoparticle stability.[33–35] This technique measures the magnitude of the electrostatic repulsion between the particles in dispersant when zeta potential is negative and attraction force when positive.[34,35] In other words, the greater the repulsion force, the more negative is the zeta potential,[33,34] and the more stable are the dispersed nanoparticles.[29] According to the zeta potential values, the LacCG-NPs appear to be more stable than the CG-NPs. Their lower zeta potential value is due to a slight increase in electrostatic repulsion and, consequently, the colloidal stability of LacCG-NPs is higher.

3.5 Circular dichroism spectroscopy analysis

Circular dichroism spectroscopy is a fast and non-destructive photometric technique. It is useful to provide information about the secondary conformational state of both proteins and polysaccharide chains. The amino acid residues in the side chains of proteins can also be monitored by measuring the CD signal.[23,24,32]

Based on the CD spectrum of CG-NPs (Fig. 4A), a well-defined minimum in ellipticity (mdeg) was exhibited at

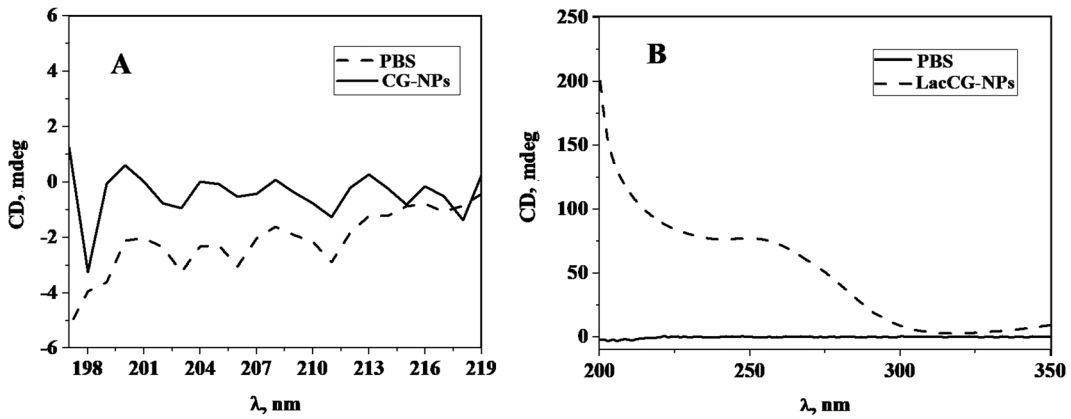

Fig. 4 Circular dichroism spectra of PBS (0.1 M pH 7.0) as blank (A and B), CG-NPs (A), and LacCG-NPs 10 : 5 (B), at 30 °C, after 1 h of incubation.

198 nm, suggesting that this sample is less structured or has a less compact organization.[32] On the other hand, LacCG-NPs (Fig. 4B) showed an inversion in the values to a positive ellipticity at 250 nm. These results indicated changes in the secondary structure of laccase, as well as its presence in LacCG-NPs, due to the interactions between the amino acid side chains of laccase,[23,24] and the side chains of the polymer[32] during the formation of LacCG-NPs. These data confirm those acquired by ATR-FTIR.

3.6 Electrochemical characterization

To understand the electrochemical behavior of the nanoparticles, we performed cyclic voltammetry and electrochemical impedance spectroscopy measurements. For this purpose, three modified glassy carbon electrodes were prepared: the first with laccase, the second with CG-NPs, and the third with LacCG-NPs. Fig. 5 shows the cyclic voltammograms and Nyquist plots of the bare and the modified glassy carbon electrode (GCE). The bare GCE produced an ineligible semi-circle, showing a linear behavior in the Nyquist plot (Fig. 5B). Nyquist plots showed a clear increase in the charge transfer resistance (R_{ct}) of LacCG-NPs, CG-NPs, and laccase films, successively.

When laccase is deposited on the electrode, a high semi-circle appears at high frequencies, with a R_{ct} of approximately 9 kΩ, which may be related to the difficulty of the electrochemical probe to reach the electrode. These results are easy to explain if we consider the isoelectric point of the enzyme (pI 4.0) and the working pH (pH 6.0). Under these experimental conditions, the enzyme has a net negative charge. Thus, an electrostatic repulsion arises between the electrochemical probe and the surface of the electrode modified with laccase. The R_{ct} value is reduced almost by half when the electrode is modified with CG-NPs (R_{ct} = 5 kΩ). Surprisingly, the LacCG-NPs modified electrode (CG : laccase ratio of 10 : 5) produced a decrease in the R_{ct} (≈4 kΩ), which means that the incorporation of laccase into the CG nanoparticles favors the electron transfer process (Fig. 5B).

These results could only be explained by considering the size of the NPs (225 nm for CG-NPs and 280 nm for LacCG-NPs). The smaller the size, the more compact is the layer formed on the electrode and the greater the difficulty of the electrochemical probe to reach the electrode. At least in part, it seems that the main effect of the nanoparticles on the electrode is that the LacNPs do not cover the electrode as much as the NPs alone, leaving holes that allow the redox probe to pass through. But this explanation would only be valid if the LacCG-NPs did not present a negative charge. This would only be possible if, during the NPs synthesis, their components suffered a structural change because of the formation of covalent bonds between them. These changes could reduce or cancel the charge of the enzyme. This hypothesis becomes consistent when we observe the spectra obtained by ATR-FTIR, which also point to a strong interaction between the –NH groups of laccase and the –OH groups of CG.

Results from cyclic voltammetry point to the same direction. When comparing the CV of the bare GCE and the modified-GCE (Fig. 5A), it is possible to observe a decrease in the oxidation and reduction currents for the latter. The highest decrease occurred in the laccase modified electrode, followed by the CG-NPs, and LacCG-NPs modified electrodes. No differences were observed in the cyclic voltammogram and Nyquist plot when the CG : enzyme proportion in the nanoparticle changed to 10 : 1 (data not shown).

3.7 Amperometric biosensor based on LacCG-NPs

LacCG-NPs were used as the biological component of an electrochemical biosensor for catechol detection. The overall process of the biosensor involves a series of steps. The first step includes, (i) the enzymatic reaction between laccase and catechol, which is oxidized to 1,2-benzoquinone in the presence of O_2, (ii) the regeneration of the reduced enzyme to its oxidized state by reacting with the oxygen in solution and, (iii) the electrochemical reduction of the benzoquinone generated in the enzymatic reaction, at +0.3 V *vs.* Ag/AgCl 3 M (Scheme 2).

The addition of catechol to the electrochemical cell containing the biosensor results in a reduction current proportional to the catechol concentration. These results confirmed the possible use of LacCG-NPs as a biological component in the design of biosensors. To find the optimal experimental conditions, different variables were studied, such as potential, pH, and temperature, using LacCG-NPs (CG : enzyme ratio of 10 : 5). For the experiment, 50 μL of nanoparticles, which correspond to approximately

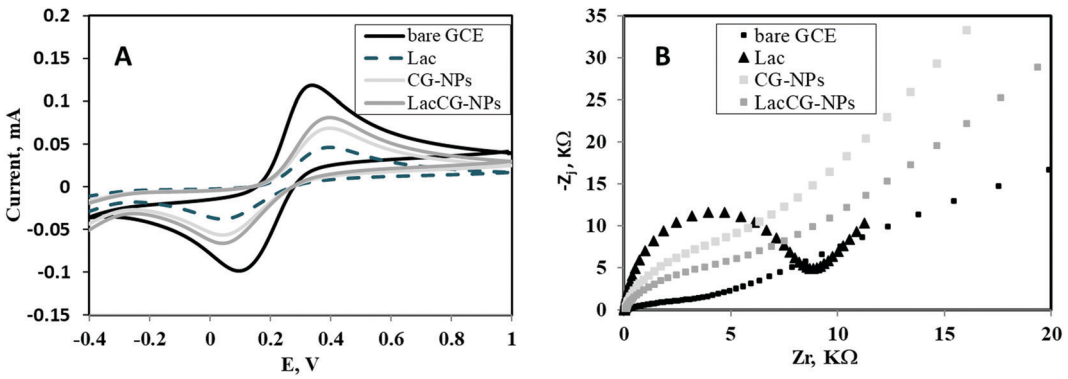

Fig. 5 Cyclic voltammograms (A) and Nyquist plot (B) of 1 mM $K_3Fe(CN)_6$ on the bare GCE and modified GCE with: Laccase (Lac), CG-NPs, and LacCG-NPs. Experimental conditions: 0.1 M PBS solution (pH 6.0), scan rate of 100 mV s^{-1}.

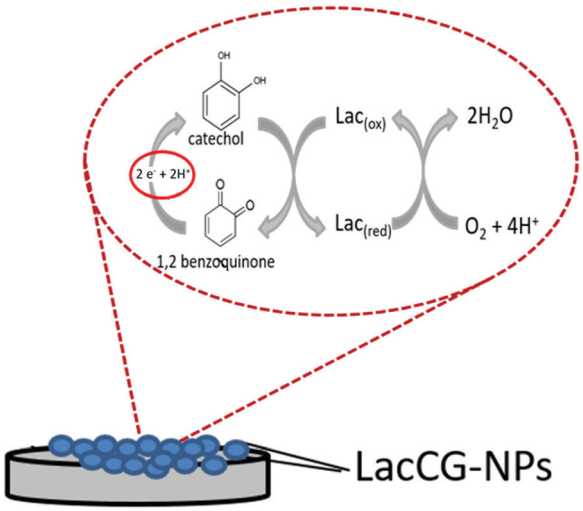

Scheme 2 Overall process to obtain the laccase-based biosensor.

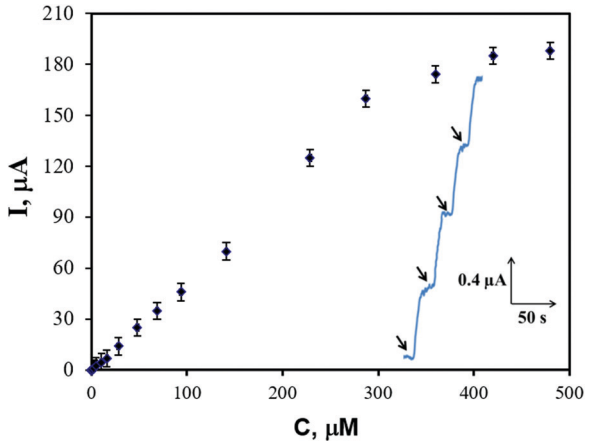

Fig. 6 Calibration curve for catechol under optimal conditions (PBS pH 7.0, 20 °C at 0.3 V). Inset: Response to the repetitive addition of catechol (1 μM).

1.25 IU of laccase, were deposited on the electrode. The influence of the applied potential was investigated in the range of −0.2 to 0.4 V *vs.* Ag/AgCl 3 M, using a 5 μM catechol solution (0.1 M PBS pH 6.0 at 25 °C). The current generated by catechol was registered until the steady state was reached. The maximum response was found at 0.3 V *vs.* Ag/AgCl 3 M and changes in any sense of the potential resulted in a decrease of the current. The pH effect on the activity of laccase was investigated in 0.05 acetate/0.05 M phosphate buffered solutions, with pH between 4.0 and 8.0, at 25 °C and 5 μM of catechol (+0.3 V *vs.* Ag/AgCl 3 M). The highest response was found at pH 7.0, which corroborates with the optimum pH reported for the free enzyme.[36] Besides, a 10% reduction in the current response was observed when the pH changed in one unity. The influence of temperature was studied in a temperature range of 5 to 35 °C, using a 5 μM catechol solution in PBS, pH 7.0 (+0.3 V *vs.* Ag/AgCl 3 M). Again, a bell-shaped curve was obtained, with a maximum response at 25 °C. Aiming to check the stability of the enzyme at different temperatures, we studied its degradation kinetics by maintaining a constant temperature for 30 minutes and seeing the evolution of the current intensity during that time. The biosensor retained 85% of its maximum response between 20 and 35 °C, but we found that the protein denaturation began at 25 °C. Thus, all the measurements were made at 20 °C.

The amount of enzyme on the electrode surface depends on two factors: the enzymatic charge of the NPs and the quantity of NPs placed on the electrode. Table 2 shows the results obtained by varying these factors. We can see that the response time depends on the load of the NPs deposited on the electrode, changing from 5.5 to 15 s when 25 and 100 μL of NPs were deposited, respectively.

We also observed a five-fold increase in the current after changing the LacCG-NPs ratio from 10 : 1 to 10 : 5 by placing 50 μL of NPs in both cases. In other words, it means that under these experimental conditions, there is a linear relationship between the enzymatic charge and the current.

The maximum response was obtained with 50 μL of LacCG-NPs (ratio 10 : 5). The current decreased as more NPs were added to the electrode. Larger amounts of NPs may form a thick film, which greatly affects the diffusion barrier and, consequently, hinders the reactions between the enzyme and the electrode.

After optimizing the factors that affect the immobilization system and the analytical properties of the biosensor, a calibration curve was prepared for catechol at the following experimental conditions: PBS pH 7.0, 20 °C, +0.3 V *vs.* Ag/AgCl 3 M, LacCG-NPs 10 : 5, and 50 μL of NPs placed on the electrode. Fig. 6 shows the calibration curve and the amperometric response obtained after the addition of catechol. The analytical characteristics obtained are descried as follows: sensitivity of 7.86 μA μM^{-1} cm^{-2}, J_{max} of 2685.7 μA cm^{-2}, linear range of 2.5 × 10^{-7}–2.0 × 10^{-4} M, and detection limit of 50 nM. A fast response time (6 s) was obtained, proving a good accessibility of catechol to the enzyme, a good diffusion of the benzoquinone to the electrode, and a fast electrode transfer reaction.

Table 2 Influence of the amount of laccase deposited on the electrode in the analytical properties of the catechol biosensor

CG : laccase ratio in the LacCG-NPs	Volume of LacCG-NPs deposited on the electrode (μL)	Amount of laccase deposited on the electrode (IU)	J_{max} (μA cm^{-2})	Response time (s)
10 : 1	50	0.25	528.2	6.1
10 : 5	25	0.625	1350.2	5.5
10 : 5	50	1.25	2571.5	6.0
10 : 5	75	1.875	2350.8	8.5
10 : 5	100	2.5	2250.3	15

Table 3 Amperometric performances of different laccase electrochemical biosensors based on organic matrices, or composites with organic polymers, for catechol detection

Biosensor[a]	Linear range (M)	Sensitivity ($\mu A\ \mu M^{-1}\ cm^{-2}$)	Detection limit (μM)	Ref.
Cu-OMC/CS	6.7×10^{-7}–1.5×10^{-5}	0.104	0.67	37
CU/CNFS/Nafion	9.9×10^{-6}–9.7×10^{-3}	0.27	1.18	38
N-OMC/PVA	3.9×10^{-7}–8.9×10^{-6}	2.41	0.31	39
rGO–PdCu NCS	5.0×10^{-6}–1.2×10^{-3} and 1.7×10^{-3}–5.1×10^{-3}	0.18 and 0.08	1.5	40
Polyaniline	3.2×10^{-6}–1.9×10^{-5}	0.47	2.07	41
rGO-GC	2.0×10^{-7}–1.5×10^{-5}	0.093	0.076	42
GR–CMF	2.0×10^{-7}–2.1×10^{-4}	0.932	0.085	43
Au–ZnO	7.5×10^{-8}–1.1×10^{-3}	0.0655	0.025	44
LacCG-NPs	2.5×10^{-7}–2.0×10^{-4}	7.86	0.05	This work

[a] CU-OMC/CS (copper-containing ordered mesoporous carbon/chitosan); CU/CNFS/Nafion (copper/carbon composite nanofibers/Nafion); N-OMC/PVA (nitrogen-doped ordered mesoporous carbon/polyvinyl alcohol); rGO–PdCu NCS (reduced graphene oxide supported palladium–copper alloyed nanocages); rGO–GC (graphene oxide–glycol chitosan); GR-CMF (graphene–cellulose microfiber); Au–ZnO micro/nanostructures.

The repeatability and reproducibility of the amperometric response were evaluated by comparing the current response of five different LacCG-NPs biosensors to a 5 μM of catechol solution. The biosensors were prepared in the same way and the procedure was performed on the same day for repeatability and in different days for reproducibility. The relative standard deviation (RSD) values obtained were 5.2% and 7.7%. These results confirm the efficiency and reproducibility of CG as a matrix for laccase immobilization. The biosensor stability was evaluated by storing it in PBS pH 7.0 at −4 °C. The response to the 5 μM catechol solution, at +0.3 V *vs.* Ag/AgCl 3 M was periodically registered. The biosensor maintained 95% of its initial signal for seven days and then a fast decay in the response was noted.

The analytical properties of the proposed catechol biosensor were compared with other recently reported biosensors based on inorganic or inorganic/organic matrices – such as chitosan, polyaniline, or cellulose microfibers, among others – used for the immobilization of laccase. The results are represented in Table 3.

The biosensor proposed in the present work has the highest sensitivity as well as one of the lowest detection limits, and a wide linear range. The use of a natural product to prepare the enzymatic nanoparticles, its easy synthesis, the immobilization efficiency, and the fast response time observed, should be highlighted. With these results, we can state that cashew gum nanoparticles are an attractive material to be used as an enzyme immobilization system for biosensors application.

4. Conclusion

This article reported, for the first time, the immobilization of an enzyme (laccase) on cashew gum nanoparticles and its application as a biological layer for biosensor development. The interaction site between the polymer and the enzyme may be related to the –OH and –NH groups of CG and laccase, respectively. Both CG-NPs and LacCG-NPs presented good size dispersion. The nanoparticles produced with the enzyme showed better colloidal stability. The electrochemical impedance spectroscopy revealed that the incorporation of laccase into the CG nanoparticles favored the electron transfer process of the redox probe when compared to CG nanoparticles alone and free laccase. LacCG-NPs were used as a biological layer in the design of an electrochemical biosensor for catechol detection, obtaining one of the lowest detection limits ever reported (50 nM) and a fast response time (6 s), which proves a good accessibility of catechol to the enzyme, a good diffusion of the benzoquinone to the electrode, and a quick electrode reaction. These results prove the applicability of these nanoparticles, based on a natural product, as the biological component in the enzyme biosensor for catechol detection.

Author contributions

Adriany das Graças Nascimento Amorim: conceptualization, data curation, formal analysis, investigation, writing – review & editing, writing – original draft. Marta Sanchez-Paniagua: conceptualization, investigation, formal analysis, writing – review & editing, writing – original draft. Taiane Maria de Oliveira: data curation, investigation. Ana Carolina Mafud: data curation, investigation. Durcilene Alves Da Silva: methodology, sources, supervision. José Roberto de Souza de Almeida Leite: conceptualization, supervision. Beatriz Lopez-Ruíz: conceptualization, supervision, writing – review & editing, writing – original draft, funding acquisition.

Conflicts of interest

The authors declare that there are no conflicts of interest.

Acknowledgements

The authors are grateful to the Complutense University of Madrid (UCM) and Federal University of Piaui (UFPI) for supporting this work.

References

1 Z. Wu, H. Li, X. Zhu, S. Li, Z. Wang, L. Wang, Z. Li and G. Chen, *Catalysts*, 2017, 7, 188.

2 M. Verrastro, N. Cicco, F. Crispo, A. Morone, M. Dinescu, M. Dumitru, F. Favati and D. Centonze, *Talanta*, 2016, **154**, 438–445.
3 S. M. S. Martínez, G. Gutiérrez-Soto, C. F. R. Garza, T. J. V. Galván, J. F. C. Cordero and C. E. H. Luna in *Applied Bioremediation – Active and Passive Approaches*, ed. Y. Patil and P. Rao, IntechOpen, 2013, ch. 15.
4 R. Reiss, J. Ihssen, M. Richter, E. Eichhorn, B. Schilling and L. Thöny-Meyer, *PLoS One*, 2013, **8**, 1–10.
5 S. Sadhasivam, S. Savitha, K. Swaminathan and F.-H. Li, *Process Biochem.*, 2008, **43**, 736–742.
6 F. Li, Z. Li, C. Zeng, Y. Hu and Y. J. Braz, *Chem. Soc.*, 2017, **28**, 960–966.
7 C. J. R. Frazão, N. H. C. Silva, C. S. R. Freire, A. J. D. Silvestre, A. M. R. B. Xavier and A. P. M. Tavares, *Eng. Life Sci.*, 2014, **14**, 500–508.
8 A. I. El-Batal, N. M. El Kenawy, A. S. Yassin and M. A. Amin, *Biotechnol. Rep.*, 2015, **5**, 31–39.
9 S. A. Ansari and Q. Husain, *Biotechnol. Adv.*, 2012, **30**, 512–523.
10 A. C. J. Oliveira, L. L. Chaves, F. O. S. Ribeiro, L. R. M. Lima, T. C. Oliveira, F. García-Villen, C. Viseras, R. C. M. Paula, P. J. Rolim-Neto, F. Hallwass, E. C. Silva-Filho, D. A. Silva, J. L. Soares-Sobrinho and M. F. R. Soares, *Carbohydr. Polym.*, 2021, **254**, 117226.
11 S. F. L. Dias, S. S. Nogueira, F. F. Dourado, A. M. Guimarães, N. A. O. Pitombeira, G. G. Gobbo, F. L. Primo, R. C. M. Paula, J. P. A. Feitosa, A. C. Tedesco, L. C. C. Nunes, J. R. S. Leite and D. A. Silva, *Carbohydr. Polym.*, 2016, **143**, 254–261.
12 S. E. Ichi, A. Zebda, J. P. Alcaraz, A. Laaroussi, F. Boucher, J. Boutonnat, N. Reverdy-Bruas, D. Chaussy, N. M. Belgacem, P. Chiquin and D. K. Martin, *Energy Environ. Sci.*, 2015, **8**, 1017–1026.
13 M. R. L. Cardial, H. C. B. Paula, R. B. C. Silva, J. F. S. Barros, A. R. Richter, F. M. Sombra and R. C. M. Paula, Pickering emulsions stabilized with cashew gum nanoparticles as indomethacin carrier, *Int. J. Biol. Macromol.*, 2019, **132**, 534–540.
14 N. A. O. Pitombeira, J. G. V. Neto, D. A. Silva, J. P. A. Feitosa, H. C. B. Paula and R. C. M. Paula, *Carbohydr. Polym.*, 2015, **117**, 610–615.
15 H. C. B. Paula, M. L. L. Rodrigues, W. L. C. Ribeiro, A. S. Stadler, R. C. M. Paula and F. O. M. S. Abreu, *J. Appl. Polym. Sci.*, 2012, **124**, 1778–1784.
16 R. R. Moraes, E. A. O. Farias, C. L. C. Carvalho, W. Cantanhêde and C. Eiras, *Int. J. Biol. Macromol.*, 2020, **153**, 118–127.
17 T. M. Silva, P. O. Santiago, L. L. A. Purcena and K. F. Fernandes, *Mater. Sci. Eng., C*, 2010, **30**, 526–530.
18 A. J. Gross, X. Chen, F. Giroud, C. Travelet, R. Borsali and S. Cosnier, *J. Am. Chem. Soc.*, 2017, **139**, 16076–16079.
19 M. T. Moreira, Y. Moldes-Diz, S. Feijoo, G. Eibes, J. M. Lema and G. Feijoo, *Appl. Sci.*, 2017, **7**, 1–11.
20 A. Amorim, A. C. Mafud, S. Nogueira, J. Ramos- Jesus, A. R. Araujo, A. Plácido, M. B. Neta, M. M. M. Alves, F. A. A. Carvalho, D. D. R. Arcanjo, S. Braun, M. S.-P. López, B. Lopez-Ruiz, C. Delerue-Matos, Y. Mascarenhas, D. Silva, P. Eaton and J. S. R. A. Leite, *J. Biomater. Appl.*, 2019, **34**, 188–197.
21 L. Deng, L. Shang, Y. Wang, T. Wang, H. Chen and S. Dong, *Electrochem. Commun.*, 2008, **10**, 1012–1015.
22 C. Liers, R. Ullrich, M. Pecyna, D. Schlosser and M. Hofrichter, *Enzyme Microb. Technol.*, 2007, **41**, 785–793.
23 J. Liu, Z. Yu, X. Liao, J. Liu, F. Mao and Q. Huang, *J. Cleaner Prod.*, 2016, **127**, 600–609.
24 S. Mojtabavi, M. R. Khoshayand, M. R. Fazeli, N. Samadi and M. A. Faramarzi, *Environ. Technol. Innovation*, 2020, **20**, 101046.
25 J. M. N. A. Bezerra, A. C. J. Oliveira, E. C. Silva-Filho, P. Severino, S. B. Souto, E. B. Souto, M. F. R. Soares and J. L. Soares-Sobrinho, *Diabetology*, 2021, **2**, 107–116.
26 Y. Vazquez-González, C. Prieto, M. F. Filizoglu, J. A. Ragazzo-Sánchez, M. Calderón-Santoyo, R. F. Furtado, H. N. Cheng, A. Biswas and J. M. Lagaron, *Carbohydr. Polym.*, 2021, **264**, 118060.
27 A. R. Richter, M. J. Carneiro, N. A. Sousa, V. P. T. Pinto, R. S. Freire, J. S. Sousa, J. F. S. Mendes, R. O. S. Fontenelle, J. P. A. Feitosa, H. C. B. Paula, F. M. Goycoolea and R. C. M. Paula, *Int. J. Biol. Macromol.*, 2020, **152**, 492–502.
28 M. C. C. Silva, M. S. F. Santos, R. D. S. Bezerra, E. A. Araújo-Júnior, J. A. Osajima, M. R. M. C. Santos, M. G. Fonseca and E. C. Silva-Filho, *Int. J. Biol. Macromol.*, 2020, **161**, 927–935.
29 I. S. Ribeiro, F. J. G. Pontes, M J. M. Carneiro, N. A. Sousa, V. P. T. Pinto, F. O. S. Ribeiro, D. A. Silva, G. S. Araújo, J. D. B. Marinho Filho, A. J. Araújo, H. C. B. Paula, J. P. A. Feitosa and R. C. M. de Paula, *Int. J. Biol. Macromol.*, 2021, **179**, 314–323.
30 P. Eaton, P. Quaresma, C. Soares, C. Neves, M. P. de Almeida, E. Pereira and P. West, *Ultramicroscopy*, 2017, **182**, 179–190.
31 J. T. Román, C. A. Fuenmayor, C. M. Z. Dominguez, D. Clavijo-Grimaldo, M. Acosta, J. E. García-Castaneda, R. Fierro-Medina and Z. J. Rivera-Monroy, *RSC Adv.*, 2019, **9**, 20432–20438.
32 A. De, D. Malpani, B. Das, D. Mitra and A. Samanta, *Carbohydr. Polym.*, 2020, **250**, 116950.
33 F. B. Araruna, T. M. Oliveira, P. V. Quelemes, A. R. A. Nobre, A. Plácido, A. G. Vasconcelos, R. C. M. Paula, A. C. Mafud, M. P. Almeida, C. Delerue-Matos, Y. P. Mascarenhas, P. Eaton, J. R. S. A. Leite and D. A. Silva, *Carbohydr. Polym.*, 2020, **241**, 115260.
34 V. Ahluwalia, S. Elumalai, V. Kumar, S. Kumar and R. S. Sangwan, *Microbial Pathogenesis*, 2018, **114**, 402–408.
35 Y. Luo, Z. Teng, Y. Y. Li, and Q. Wang, *Carbohydr. Polym.*, 2015, **122**, 221–229.
36 Y. Y. Wan, R. Lub, L. Xiao, Y. M. Du, T. Miyakoshi, C. L. Chen, C. J. Knill and J. F. Kennedy, *Int. J. Biol. Macromol.*, 2010, **47**, 488–495.
37 X. Xu, M. Guo, P. Lu and R. Wang, *Mater. Sci. Eng., C*, 2010, **30**, 722–729.

38 J. Fu, H. Qiao, D. Li, L. Luo, K. Chen and Q. Wei, *Sensors*, 2014, **14**, 3543–3556.
39 M. Guo, H. Wang, D. Huang, Z. Han, Q. Li, X. Wang and J. Chen, *J. Sci. Technol. Adv. Mater.*, 2014, **15**, 035005.
40 L. P. Mei, J. J. Feng, L. Wu, J. Y. Zhou, J. R. Chen and A. J. Wang, *Biosens. Bioelectron.*, 2015, **74**, 347–352.
41 M. Nazari, S. Kashanian and R. Rafipour, *Spectrochim. Acta, Part A*, 2015, **145**, 130–138.
42 A. Boujakhrout, S. Jimenez-Falcao, P. Martinez-Ruiz, A. Sanchez, P. Diez, J. M. Pingarron and R. Villalonga, *Analyst*, 2016, **141**, 4162–4169.
43 S. Palanisamy, S. K. Ramaraj, S. M. Chen, T. C. K. Yang, P. Yi-Fan, T. W. Chen, V. Velusamy and S. Selvam, *Sci. Rep.*, 2017, **7**, 41214.
44 T. Liu, Q. Zhao, Y. Xie, D. Jiang, Z. Chu and W. Jin, *Biosens. Bioelectron.*, 2020, **156**, 112145.